# Engineered Eglin c Variants Inhibit Yeast and Human Proprotein Processing Proteases, Kex2 and Furin[†]

Tomoko Komiyama and Robert S. Fuller*

*Department of Biological Chemistry, University of Michigan Medical School, Room 5413 Medical Science I, 1301 East Catherine, Ann Arbor, Michigan 48109*

*Received August 11, 2000; Revised Manuscript Received October 6, 2000*

ABSTRACT: We engineered eglin c, a potent subtilisin inhibitor, to create inhibitors for enzymes of the Kex2/furin family of proprotein processing proteases. A structural gene was synthesized that encoded "$R_1$-eglin", having Arg at $P_1$ in the reactive site loop in place of $Leu_{45}$. Ten additional variants were created by cassette mutagenesis of $R_1$-eglin. These polypeptides were expressed in *Escherichia coli*, purified to homogeneity, and their interactions with secreted, soluble Kex2 and furin were examined. $R_1$-eglin itself was a modest inhibitor of Kex2, with a $K_a$ of $\sim 10^7$ $M^{-1}$. Substituting Arg (in $R_4R_1$-eglin) or Met (in $M_4R_1$-eglin) for $Pro_{42}$ at $P_4$ created potent Kex2 inhibitors exhibiting $K_a$ values of $\sim 10^9$ $M^{-1}$. $R_4R_1$-eglin inhibited furin with a $K_a$ of $4.0 \times 10^8$ $M^{-1}$. Introduction of Lys at $P_1$, in place of Arg in $R_4R_1$-eglin reduced affinity only ~3-fold for Kex2 but 15-fold for furin. The stabilities of enzyme−inhibitor complexes were characterized by association and dissociation rate constants and visualized by polyacrylamide gel electrophoresis. $R_4R_1$-eglin formed stable 1:1 complexes with both Kex2 and furin. However, substitution of Lys at $P_2$ in place of $Thr_{44}$ resulted in eglin variants that inhibited both Kex2 and furin but which were eventually cleaved (temporary inhibition). Surprisingly, $R_6R_4R_1$-eglin, in which Arg was substituted for $Gly_{40}$ in $R_4R_1$-eglin, exhibited stable, high-affinity complex formation with Kex2 ($K_a$ of $3.5 \times 10^9$ $M^{-1}$) but temporary inhibition of furin. This suggests that enzyme-specific interactions can alter the conformation of the reactive site loop, converting a permanent inhibitor into a substrate. Eglin variants offer possible avenues for affinity purification, crystallization, and regulation of proprotein processing proteases.

Numerous secretory peptides and proteins that undergo processing at basic residue sites during their transit through late compartments of the secretory pathway are thought to be cleaved by members of the kexin/furin family of eukaryotic processing proteases (*1*). In yeast, Kex2 protease (kexin EC 3.4.21.61) cleaves the "polyprotein" precursor pro-α-factor at the carboxyl side of Lys−Arg sites and the precursor of the disulfide-linked heterodimeric killer toxin at Arg−Arg and Lys−Arg sites. Kex2 is thus required for both α-specific mating and for killer toxicity (*2*). Mammalian Kex2 homologues include furin, PC1/3, PC2, PC4, PACE4, PC5/PC6, and LPC/PC7/PC8 (*1*). These molecules exhibit diverse temporal and spatial patterns of expression during development as well as differential localization within individual cells. PC1/3 and PC2, which are expressed in neuronal and neuroendocrine cells, are sorted into nascent secretory granules and appear to account for the processing of neuropeptide precursors and prohormones in the regulated secretory pathway (*1*, *3*−*5*). Although important for normal endocrine function, PC1/3 and PC2 appear not to be essential for mammalian development, whereas another Kex2 homologue, furin, is required at an early embryonic stage of mouse development (*6*).

Furin is expressed nearly ubiquitously in mammalian tissues and is localized to the trans Golgi network (TGN),[1] endosomes, and plasma membrane where it is thought to process substrates (*7*). Likely endogenous substrates of furin include precursors of growth factors and growth factor receptors, metalloprotease precursors, and coagulation factor precursors, among others (*7*). Furin, and possibly other members of the kexin/furin family, are also thought to play important roles in bacterial and viral pathogenesis. Several bacterial toxins, including *Pseudomonas* exotoxin A, diphtheria toxin, and anthrax protective antigen, are synthesized as precursors that undergo processing by a host cell protease at furin-type cleavage sites (Arg−Xaa−Xaa−Arg↓) (*7*). Purified furin has been shown to cleave several bacterial protoxins and tissue culture cell lines that lack a gene encoding furin are resistant to toxins (*8*−*11*). Additionally, the viral envelope glycoproteins of numerous lipid-enveloped viruses require processing by a furin-like enzyme (*7*). These include the glycoproteins of many pathogenic human and animal viruses that include the fowl plague influenza virus, Semliki forest virus, Newcastle disease virus, parainfluenza viruses, measles, herpes viruses, Ebola virus, and various retroviruses (*12*−*23*).

Although knocking out the *fur* gene in mouse results in developmental lethality (*6*), the viability of furin-deficient

[†] This work was supported by NIH GM39697 (R.S.F.).

* To whom correspondence should be addressed.

[1] Abbreviations: trans Golgi network (TGN); AMC, 7-amino-4-methylcoumarin; MUTMAC, 4-methylumbelliferyl *p*-(*N*,*N*,*N*-trimethylammonium)cinnamate; TUG, transverse urea gradient; NPGB, *p*-nitrophenyl *p*-guanidinobenzoate hydrochloric acid; PAGE, polyacrylamide gel electrophoresis; MALDI, matrix-assisted laser desorption/ionization; MES, 2-(*N*-morpholino)ethanesulfonic acid; CI2, chymotrypsin inhibitor 2.

10.1021/bi001907c CCC: $19.00 
Published on Web 11/10/2000

cell lines (*24*, *25*) suggests that this host processing pathway might offer a novel target for the development of broad-spectrum drugs for treatment of acute bacterial and viral infection. Peptidyl chloromethyl ketones have been synthesized that inhibit both Kex2 (*26*) and furin (*27*). Acylated peptidylchloromethyl ketones have been shown to inhibit furin-type processing in cell culture (*28*). However, concerns about toxicity limit the possible therapeutic applications of these molecules. Several protein inhibitors of processing proteases have been described, including engineered ovomucoid third-domain inhibitors (*29*), serpin variants (*30*, *31*), and "kexstatin," a molecule related to the *Streptomyces* subtilisin inhibitor (*32*). Of these molecules, the genetically engineered serpin $\alpha_1$-PDX is the best characterized and most specific protein inhibitor of furin (*30*). Inhibition of processing by $\alpha_1$-PDX in vivo has been demonstrated both by expressing the $\alpha_1$-PDX gene in target cells and by adding the purified protein to tissue culture media (*21*, *30*, *33*). However, the large size (~400 a.a.) and relative instability of serpin family inhibitors may hamper the development of these molecules for therapeutic use.

We have created a new family of genetically engineered inhibitors of proprotein processing proteases based on eglin c, a polypeptide protease inhibitor from the leech *Hirudo medicinalis*. The choice of eglin c as a template for building new inhibitors was guided by several considerations. First, eglin c, like most members of the potato inhibitor 1 family (*34*−*36*), lacks disulfide bonds, unlike inhibitors of the Kunitz family (e.g., BPTI) or the Kazal (ovomucoid) family (*37*), facilitating robust expression. Second, despite its small size (70 a.a.) and the absence of disulfide bonds, eglin c is thermostable ($T_M \sim 86$ °C) (*38*). Third, eglin c is a potent inhibitor of degradative subtilisins. Indeed, crystal structures of several subtilisin−eglin c complexes have been solved (*39*−*42*). Finally, NMR studies have shown that the potato inhibitor 1 family has relatively flexible reactive site loops that may increase the ability of eglin c-based inhibitors to adapt to distinct structural features of the catalytic binding regions of new target enzymes (*43*, *44*). Thus, we had a reasonable expectation that incorporation of appropriate sequence alterations within the eglin c reactive site loop would result in inhibitors that would dock well with the subtilisin-related processing enzymes.

The catalytic domains of the kexin/furin processing proteases are homologous to the degradative subtilisins, and, as a result, broad features of substrate recognition are conserved even though specificity, per se, is not. We have studied the specificities of secreted, soluble forms of Kex2 (ssKex2, ref *45*) and furin (ssfurin, ref *46*) using sets of fluorogenic peptide substrates (*45*, *47*, *48*). These studies have provided us a detailed picture of enzyme−substrate interactions for these two processing enzymes. The processing enzymes conserve the propensity, found in degradative subtilisins, to recognize the $P_1$, $P_2$, and $P_4$ residues of substrates (*49*, *50*). However, the nature of recognition at the sites differs markedly. The degradative enzymes exhibit generic specificity, tending to prefer hydrophobic residues at $P_1$ and $P_4$ and small residues at $P_2$. In contrast, Kex2 and furin tend to prefer basic residues at these positions. The two enzymes exhibit high selectivity for Arg at $P_1$ (100- to 10 000-fold) (*45*, *47*). Kex2 also exhibits stringent selection for the $P_2$ side chain (Lys or Arg) and a less, but still measurable, selectivity for the $P_4$ residue (basic or aliphatic) (refs *47* and *51*; D. J. Krysan and R. S. Fuller, unpublished data). In contrast, furin exhibits stringent specificity for Arg at $P_4$ and more relaxed specificity for a basic residue at $P_2$ (*21*, *48*, *52*). In addition, furin is selective for Arg at $P_6$ (*21*, *48*, *52*), whereas Kex2 is indifferent to the $P_6$ residue (*48*). In the current work, substitutions were introduced into the reactive site loop of eglin c at the $P_1$ ($Leu_{45}$), $P_2$ ($Thr_{44}$), $P_4$ ($Pro_{42}$), and $P_6$ ($Gly_{40}$) positions. Ten reactive site variants were generated by cassette mutagenesis of a synthetic eglin gene that had Arg at $P_1$. A "wild-type" eglin c with Leu at $P_1$ was created to serve as a control. Several of the engineered eglin c variants were found to bind tightly and form stable, reversible complexes with both Kex2 and furin at a stoichiometry of 1:1.

## MATERIALS AND METHODS

*Reagents.* All restriction enzymes, Vent DNA polymerase and DNA modifying enzymes were from New England BioLabs. NuSieve GTG agarose was from FMC. The pET27b(+) vector was from Novagene. A chromogenic substrate, H−D-Ile−Pro−Arg-pNA, was from DiaPharma (OH). Fluorogenic substrates, Boc-Pro−Val−Arg-MCA, Boc-Arg−Val−Arg−Arg-MCA, and pyrArg−Thr−Lys−Arg-MCA were from Bachem Bioscience. 4-Methylumbelliferyl p-(*N*,*N*,*N*-trimethylammonium)cinnamate (MUTMAC) was from Sigma. Oligonucleotides (University of Michigan DNA Core Facility) were purified by PAGE in 7 M urea. Secreted, soluble Kex2 (hereafter, "Kex2") was purified and active-site titrated as described (*43*, *51*). Serum-free media adopted insect cells (sf-9 cells) were from Gibco BRL. Human neutrophil elastase, plasma kallikrein, and plasmin were from Athens Research and Technology. The micro BCA assay kit was from Pierce.

*Expression and Purification of Secreted Soluble Human Furin.* Secreted, soluble human furin (hereafter, "furin") was expressed using the BAC-TO-BAC Baculovirus expression system (Gibco BRL). Plasmid pUN70-fur-595 (*46*), encoding the catalytic and P-domains of human furin, was cloned into pFAST-BAC vector. Sf-9 cells were infected with the recombinant bacmid (pFAST-BAC fur-595) for 72 h to make recombinant baculovirus stock, and the virus stock was amplified through two subsequent rounds of infection. Furin expression was monitored by measuring hydrolysis by conditioned medium of Boc-Arg−Val−Arg−Arg-MCA. Media were pooled 48 h after infection and subjected to continuous flow dialysis using a 50 kDa cutoff Prep/Scale-TFF cartridge (Millipore), exchanging the enzyme into 10 mM Tris-HCl, pH 8.0, 1 mM $CaCl_2$. Furin was purified as described previously (*46*) with the following modifications. After adsorption of furin from dialyzed medium onto Q-Sepharose, elution was achieved with a linear NaCl gradient from 0.05 to 0.35 M (peak at 0.15 M). Pooled peak fractions were concentrated and dialyzed using pressure dialysis on an Amicon XM-50 membrane. Final purification was performed by chromatography on a Bio-Scale Q20 column (Bio-Rad) using a Perkin-Elmer HPLC system. Furin was eluted with a linear NaCl gradient from 0.05 to 0.35 M in 10 mM Tris-HCl, pH 8.0. Enzyme in the peak fraction, which eluted at 0.2 M NaCl, was concentrated and exchanged into buffer containing 20 mM NaMES, pH 7.0, 1 mM $CaCl_2$, and 10% glycerol, and stored at −80 °C.


FIGURE 1: Synthetic gene encoding $Arg_{45}$-eglin. The high abundance *E. coli* codons were used to design a synthetic nucleotide sequence for $Arg_{45}$-eglin, following the published DNA sequence of eglin c (*53*). *Nde*I, *Nco*I, and *Bam*HI sites were designed for cloning into the pET27b(+) vector. *Aat*II and *Bgl*II sites were introduced for cassette mutagenesis of the reactive site loop. For protein expression, the *Aat*II site was silenced by mutating CGA to CGT for the Arg45 ($P_1$ position). The N-terminal three amino acid residues (MSM) differ from that (TGF) of the naturally occurring eglin c. Target residues for site-directed mutagenesis, $Gly_{40}$ ($P_6$), $Pro_{42}$ ($P_4$), $Thr_{44}$ ($P_2$), and $Leu_{45}$ ($P_1$), are indicated in bold and are underlined.

Table 1: Summary of MWs of Eglin Variants Determined by MALDI Mass Spectrometry[a]

| eglin variant | $P_6$ | $P_5$ | $P_4$ | $P_3$ | $P_2$ | $P_1$ | $MW_{obsd}$ | $MW_{calcd}$ |
|---|---|---|---|---|---|---|---|---|
| $L_1$- | Gly | Ser | Pro | Val | Thr | Leu | 7932 | 7931 |
| $R_1$- | − | − | − | − | − | Arg | 7970 | 7974 |
| $R_4$- | − | − | Arg | − | − | − | 7988 | 7990 |
| $M_4R_1$- | − | − | Met | − | − | Arg | 8011 | 8008 |
| $R_4R_1$- | − | − | Arg | − | − | Arg | 8034 | 8033 |
| $M_4K_1$- | − | − | Met | − | − | Lys | 7981 | 7983 |
| $R_4K_1$- | − | − | Arg | − | − | Lys | 8006 | 8006 |
| $R_6R_4R_1$- | Arg | − | Arg | − | − | Arg | 8137 | 8133 |
| $K_2R_1$- | − | − | − | − | Lys | Arg | 8004 | 8001 |
| $M_4K_2R_1$- | − | − | Met | − | Lys | Arg | 8038 | 8035 |
| $R_4K_2R_1$ | − | − | Arg | − | Lys | Arg | 8062 | 8060 |

[a] The N-terminal sequences of the eglin variants were determined to be Ser−Met−Gly−Ser−Glu−Leu-, implying removal of the N-terminal Met residue; therefore, calculated MWs assume the absence of the N-terminal Met. Residues identical to $L_1$-eglin are indicated by "−".

*Gene Synthesis and Expression of $R_1$-Eglin.* Standard methods for molecular biology and bacterial cell growth and transformation were as described (*54*). A synthetic gene encoding eglin c with Arg in place of $Leu_{45}$ was designed using a previously published eglin c synthetic gene as a guide (*55*). The synthetic gene (231 bp) was divided into six fragments of ~55 bp (Figure 1). Assembly of the paired segments was performed by PCR using Vent DNA polymerase. The final gene product was subcloned into pBS-$SK^+$ and sequenced. *Nde*I and *Bam*HI sites permitted subsequent subcloning into expression vector pET27b(+). *Aat*II and *Bgl*II restriction sites were introduced to permit cassette mutagenesis of the reactive site loop from $Arg_{45}$ ($P_1$) to $Gly_{40}$ ($P_6$) (Figure 1). Using these sites, a series of substitutions was made at the $P_2$, $P_4$, and $P_6$ positions in the $R_1$-eglin. A gene encoding a recombinant eglin having the reactive site sequence of naturally occurring eglin c was also constructed. The product of this gene was termed "$L_1$-eglin". $L_1$-eglin ("wild-type eglin") expressed in this study has the N-terminal sequence SMGSELK, in contrast to the naturally occurring eglin c N-terminal sequence of TEFGSELK. Other variants were designated by according to the substitutions made at the $P_1$, $P_2$, $P_4$, and $P_6$ positions (see Table 1). Automated DNA sequencing was used to confirm each construction.

*Expression and Purification of Eglin c Variants.* Expression vectors were transformed into bacterial host strain BL21-(DE3) as described (*56*). Eglin expression was induced with isopropylthiogalactoside when cells grown in LB medium containing 30 $\mu$M kanamycin reached an $OD_{600}$ of 0.4. The harvested cells were washed with 150 mM NaCl and frozen (−80 °C). Surprisingly, although the synthetic eglin c gene encoded no signal peptide, washing thawed cells with 50 mM Tris-HCl (pH 8) containing 2 mM EDTA released the eglin proteins quantitatively without extensive cell lysis. The Tris extract was subjected to Q-Sepharose ion exchange chromatography in 20 mM Tris-HCl (pH 8.0) to remove medium contaminants. The proteins were purified by S-Sepharose chromatography in 20 mM sodium acetate (pH 5.0) and eluted with a linear NaCl gradient, 0.0 to 0.6 M NaCl. Purified eglin variants were judged to be homogeneous by SDS−PAGE. The percentage of active species was determined to be ≥99.5 by comparing results of inhibition and protein (BCA) assays. Eglin inhibitory activity was titrated as described below. Total yields of purified proteins were ~7 mg from 100 mL of bacterial culture. Molecular weights of eglin variants were determined by MALDI mass spectrometry.

*Protein Analysis.* Purified proteins were analyzed by nondenaturing, SDS-, and transverse urea gradient (TUG)-PAGE. The 2-amino-2-methyl-1,3-propanediol buffer system was used for all PAGE analysis (*57*). TUG gels (6% acrylamide, w/v) contained a continuous transverse 0.0 to 8.0 M urea gradient and were cast as described (*58*, *59*). For further confirmation of the protein products, N-terminal sequence determination and isoelectric focusing PAGE analysis were performed. For N-terminal sequence determination (University of Michigan protein core facility), purified proteins were run in PAGE and transferred to poly(vinylidene difluoride) membranes (*60*).

*Active-Site Titration.* Active site titration of Kex2 was performed as described (*45*). Furin was titrated using an RQF-3 rapid-quenched flow apparatus (Kintech Corp.) by measuring the initial burst of AMC product from hydrolysis of pyrArg−Thr−Lys−Arg-MCA (307 $\mu$M) at 21 °C with reaction times ranging from 4 ms to 60 s. Active-site titration of trypsin was done using the chromogenic substrate *p*-nitrophenylguanidinobenzoate (NPGB) (*61*).

*Inhibition Assays.* Purified eglin variants were titrated with active-site titrated Kex2 or trypsin by measuring hydrolysis of chromogenic substrates H-D-Ile−Pro−Arg-pNA or Boc-Arg-pNA on a Uvikon spectrophotometer (Kontron) at 21 °C in Kex2 assay buffer: 200 mM Bistris containing 1 mM $CaCl_2$, 0.1% (v/v) Triton-X-100, or furin assay buffer: 20 mM NaMES containing 1 mM $CaCl_2$, 0.1% (v/v) Triton-X-100. $R_1$-, $M_4K_1$-, and $R_4K_1$-variants were incubated with trypsin (0.5 $\mu$M) until the inhibition reached equilibrium. Bz-Arg-pNA hydrolysis by residual trypsin activity was monitored. $M_4R_1$-, $R_4R_1$-, and $R_6R_4R_1$-variants were titrated with the active site titrated Kex2 (0.1 $\mu$M). All titration mixtures were analyzed by SDS−PAGE after titration. When no cleavage products of the inhibitors were detected, the accuracy of the titration was confirmed. Three eglin variants, $K_2R_1$-, $M_4K_2R_1$-, and $R_4K_2R_1$-eglin were not titratable with tested enzymes. For these inhibitors, protein concentration determined by BCA assay was used as the inhibitor concentration. $L_1$-eglin was titrated with chymotrypsin which was active-site titrated with MUTMAC.

*Determination of Kinetic Constants.* To measure the affinity of titrated eglin variants for furin and Kex2, the enzymes were diluted to concentrations ranging from 0.5 to 2 nM in either Kex2 assay buffer or furin assay buffer and incubated with appropriate dilutions of the eglin variants made in the same buffer, for 45 min to 1 h at 21 °C. 100- to 200-$\mu$L aliquots of reaction mixtures were transferred into triplicate wells of opaque 96-well plates (Costar), and residual enzyme activity was measured by following the hydrolysis of a fluorogenic substrate. For furin, 2.0 $\mu$M Boc-Arg−Val−Arg−Arg-MCA was used. For Kex2 either 15 $\mu$M Boc-Pro−Val−Arg-MCA or 2.1 $\mu$M Boc-Arg−Val−Arg−Arg-MCA was used. Fluorescence was recorded for least 20 min using an fmax fluorescence microtiter plate reader (Molecular Devices) with a 360-nm excitation filter and a 480-nm emission filter. Reactions were linear for the duration of the recording. Data from multiple measurements were averaged and graphically analyzed (KaleidaGraph) with eq 1 (*62*) to determine the equilibrium association constant, $K_a$.

$$[E] = E_0 - 1/2\{[E_0] + [I_0] + 1/K_a - \sqrt{([E_0] + [I_0] + 1/K_a)^2 - 4[E_0][I_0]}\} \quad (1)$$

where

$$K_a = \frac{[EI]}{[E][I]}$$

where $[E_0]$, $[I_0]$ are the total concentrations of enzyme and inhibitor, and $[E]$, $[I]$, and $[EI]$ are the free concentrations of enzyme, inhibitor, and the complex at equilibrium.

The association rate constant ($k_{on}$) was determined by recording inhibition progress curves, monitoring hydrolysis of a substrate (Boc-Arg−Val−Arg−Arg-MCA for furin and Kex2) as a function of time after adding enzyme to a solution containing an inhibitor and the substrate. Progress curves were graphically analyzed by fitting data to eqs 2 and 3 using KaleidaGraph (*63*, *64*). $F$ is fluorescence measured, $v_0$ is the

$$F = v_s t + (v_0 - v_s)(1 - e^{-k_{obs}t})/k_{obs} + F_0 \quad (2)$$

$$k_{on} = (k_{obs}/I)(1 + S/K_m) \quad (3)$$

initial uninhibited rate, $v_s$ the final steady-state rate, and $k_{obs}$ is the observed, first-order relaxation rate constant. $S$ is the substrate concentration, and $E_0$ is the total enzyme concentration. Dissociation rate constants ($k_{off}$) were calculated from the relationship: $k_{off} = k_{on}/K_a$.

## RESULTS

*Characterization of Eglin Variants.* The parent eglin c construction was based on a synthetic eglin c gene optimized for *Escherichia coli* codon usage (*55*). Consistent with this, expression of all 11 eglin c variants using the pET vector system resulted in extremely high yields of the recombinant proteins. Unexpectedly, although the constructs did not incorporate a secretory signal peptide, we found that the eglin c variants were quantitatively recovered from the cells by osmotic shock (Figure 2). Eglin c polypeptides were passed through Q-Sepharose to remove nucleotides and nucleic acids and subjected to ion-exchange chromatography on S-Sepharose, yielding homogeneous product as judged by

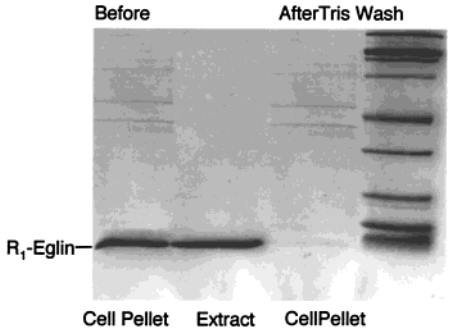


FIGURE 2: SDS−PAGE analysis of eglin variant expression: extraction of $R_1$-eglin from BL21(DE3) cells. Cells were grown, eglin expression was induced and cells were harvested, washed, and frozen as described in Materials and Methods. Samples were boiled in SDS sample buffer containing 1% SDS and 20 mM DTT for five min. 5−15% polyacrylamide gradient gels were run and stained with Coomassie blue R250. Lane 1, whole cells resuspended in 4 M urea prior to SDS−PAGE. Lane 2, protein extracted from cells with 50 mM Tris, pH 8, containing 2 mM EDTA. Lane 3, cell pellet resuspended in 4 M urea after protein extraction. Lane 4, protein standards (6−200 kDa). Samples in lanes 1−3 represent material from identical numbers of cells.

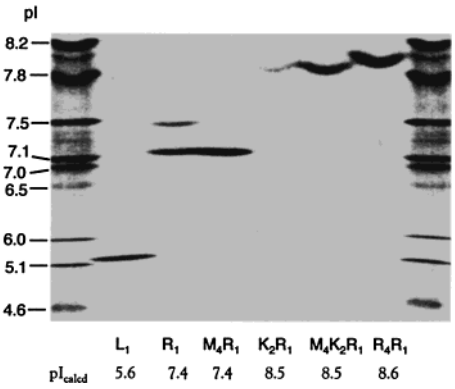


FIGURE 3: Isoelectric focusing PAGE of eglin variants. Lanes 1 and 8, p*I* standards. Lanes 2−7, eglin variants as indicated. Calculated p*I* values are shown below lanes. The slowly migrating band in lane 3 represents a contaminant that was removed with further purification.

SDS−PAGE (data not shown), isoelectric focusing PAGE (Figure 3), N-terminal sequence analysis (Materials and Methods), and MALDI mass spectrometry (Table 1). Substitutions of positively charged residues in the reactive site loop of individual eglin c variants had the predicted effects on p*I* (Figure 3). TUG-PAGE analysis showed that all variants remained folded, like eglin c itself, in urea concentrations up to ~8 M (Figure 4). The concentration of the active form of the inhibitors was determined by titration with active-site titrated proteases (Materials and Methods). Equilibrium association constants for the interactions of the eglin variants with Kex2 and furin were determined (Figure 5 and Table 2).

*$P_1$ and $P_4$ Substitutions Create Eglin c Variants with High Affinity for Furin and Kex2.* Genes encoding eglin variants with substitutions at the $P_1$ and $P_4$ positions were created, the variant proteins were purified, and their affinities for furin and Kex2 were determined by examining inhibitory potency. Substitution of a single Arg for Leu at $P_1$, in $R_1$-eglin, had little effect on furin affinity (2.5-fold increase) but resulted in a dramatic increase ($10^4$-fold) in affinity for Kex2. The substitution of Met for Pro at $P_4$, resulting in $M_4R_1$-eglin,

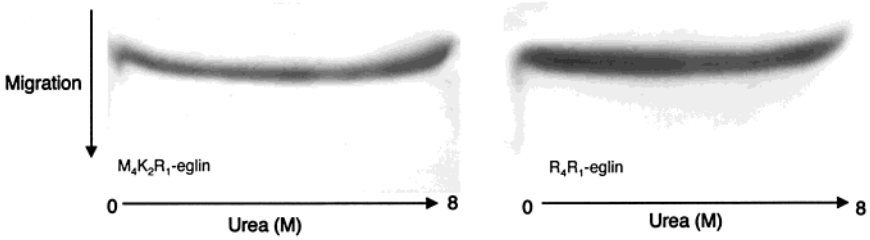


FIGURE 4: TUG−PAGE analysis of $M_4K_2R_1$-eglin and $R_4R_1$-eglin. 7% polyacrylamide gels contained a linear gradient of urea from 0 to 8 M. Electrophoresis conditions otherwise were identical to nondenaturing PAGE.

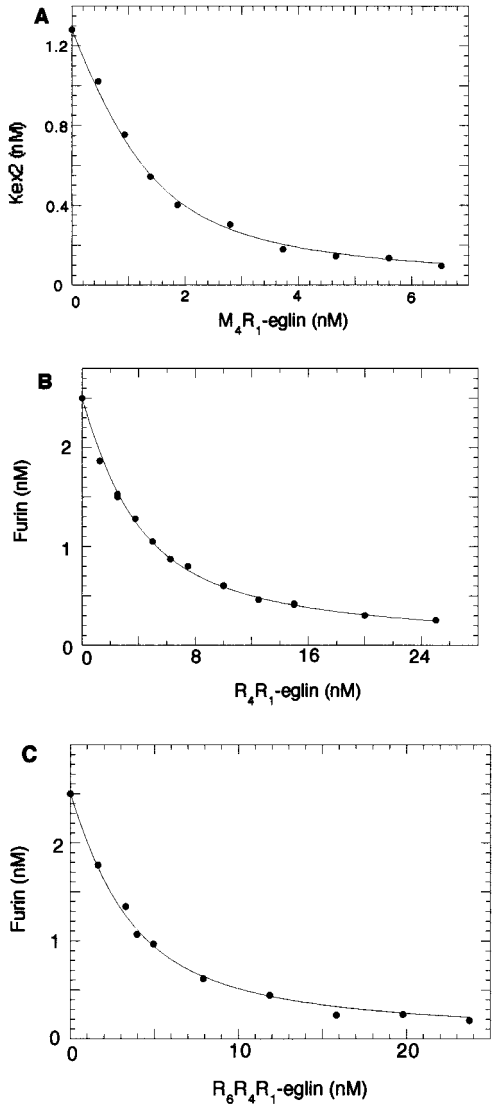


FIGURE 5: Inhibition curves of Kex2 with $M_4R_1$-eglin (A), furin with $R_4R_1$-eglin (B), and furin with $R_6R_4R_1$-eglin (C). The proteases were incubated with the inhibitors for 45 min at 21 °C in either the Kex2 or furin assay buffers described in Materials and Methods. Residual activity of the proteases was measured with Boc-Arg−Val−Arg−Arg-MCA (2 $\mu$M) on an fmax fluorescence microtiter plate reader (Molecular Devices). Plots were fitted graphically to eq 1 using Kaleidagraph 3.0.

increased furin affinity 15-fold. However, once again, the substitution had a much larger effect on Kex2 affinity, increasing the $K_a$ 88-fold. Relative to $L_1$-eglin (wild-type reactive site loop), $M_4R_1$-eglin exhibited $1.5 \times 10^6$-fold increased affinity for Kex2 but only 33-fold increased affinity for furin. Unlike Kex2, which appears to bind $P_4$ basic and aliphatic residues with comparable affinity (*51*), furin exhibits

Table 2: Equilibrium Association Constants $K_a$ ($M^{-1}$) of Eglin Variants with Kex2 and Furin[a]

| | $K_a$ ($M^{-1}$) | |
|---|---|---|
| eglin variant | Kex2 | furin |
| $L_1$- | $\approx 2 \times 10^3$ | $8.7 \times 10^3$ |
| $R_1$- | $3.3 \times 10^7$ | $1.9 \times 10^4$ |
| $R_4$- | $1.0 \times 10^4$ | $1.8 \times 10^4$ |
| $M_4R_1$- | $2.9 \times 10^9$ | $2.8 \times 10^5$ |
| $R_4R_1$- | $1.1 \times 10^9$ | $4.0 \times 10^8$ |
| $R_4K_1$- | $4.0 \times 10^8$ | $2.6 \times 10^7$ |
| $M_4K_1$- | $2.2 \times 10^8$ | $6.0 \times 10^4$ |
| $R_6R_4R_1$- | $3.5 \times 10^9$ | $4.9 \times 10^{8}$* |
| $K_2R_1$- | $1.5 \times 10^{9}$* | $9.6 \times 10^{6}$* |
| $M_4K_2R_1$- | $1.7 \times 10^{9}$* | $1.2 \times 10^{7}$* |
| $R_4K_2R_1$- | $2 \times 10^{9}$* | $2 \times 10^{9}$* |

[a] $K_a$ values were determined under standard assay conditions for the two enzymes: Kex2, 200 mM Bistris, pH 7.27, containing 1 mM $CaCl_2$, and 0.1% Triton X-100; furin, 20 mM NaMES, pH 7.0, containing 1 mM $CaCl_2$ and 0.1% Triton X-100. Asterisks (*) indicate temporary inhibition. Note that $R_6R_4R_1$-eglin is a stable inhibitor of Kex2 and a temporary inhibitor of furin.

a high degree of selectivity for Arg at $P_4$ (*48*). Indeed, substitution of Arg for Met at $P_4$ in $M_4R_1$-eglin, creating $R_4R_1$-eglin, substantially increased affinity for furin (1430-fold) but only slightly altered Kex2 affinity (2.5-fold decrease). Overall, $R_4R_1$-eglin exhibited a $4.6 \times 10^4$-fold higher affinity for furin than $L_1$-eglin. High-affinity binding of $R_4R_1$-eglin to furin involves highly cooperative binding of the $P_1$ and $P_4$ Arg residues because, as shown in Table 2, the presence of Arg at only $P_1$ (mentioned above) or at $P_4$ (in $R_4L_1$-eglin) resulted in only a 2−3-fold enhancement of affinity relative to $L_1$-eglin. Kex2, on the other hand, exhibited high affinity for eglin with Arg at $P_1$ alone but substitution of Arg alone at $P_4$ (Table 2) only slightly increased affinity (5-fold).

Although the two enzymes exhibited distinct patterns of inhibition by this set of eglin molecules, both enzymes exhibited a high degree of affinity ($K_i$ ca. $10^{-9}$ M) for eglin variants with appropriate substitution at just the $P_1$ and $P_4$ sites. To examine the stability and stoichiometry of complexes formed between $P_4P_1$ variant eglins and Kex2 and furin, enzyme−inhibitor mixtures were analyzed by native and denaturing PAGE. In Figure 6, panel A, it can be seen that in native PAGE, a stoichiometric complex of Kex2 and $M_4R_1$-eglin formed after a 15-min preincubation. This complex migrated more rapidly than either molecule alone, indicating a significant decrease in p$K_a$ upon complex formation. In SDS−PAGE, the complex dissociated into free protease and intact inhibitor (Figure 6, panel B). Complexes formed between stoichiometric amounts of Kex2 or furin and eglin variants were analyzed by SDS−PAGE after overnight incubation at room temperature. With the exception

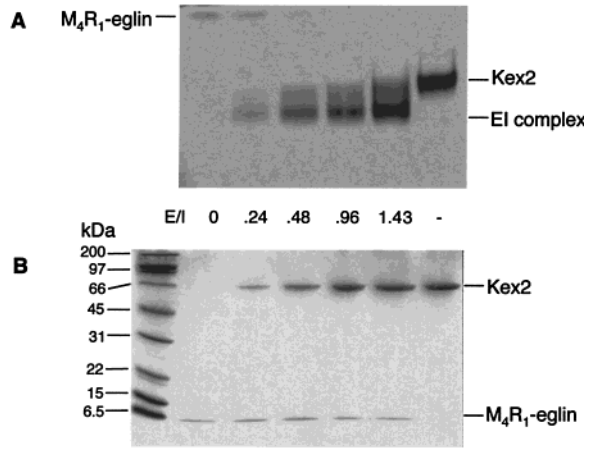


FIGURE 6: Native and SDS−PAGE analyses of the reaction between $M_4R_1$-eglin (I) and Kex2 (E). $M_4R_1$-eglin (64 pmol) was incubated with Kex2 under the E/I ratio in the range of 0 to 1.43 for 15 min at 21 °C. The samples were divided into two parts and analyzed by nondenaturing-PAGE (A) and by SDS−PAGE (B). For SDS−PAGE, the reaction was stopped with 10% TCA. The TCA precipitates were washed with 10% TCA solution and ethanol−acetone mixture (1:1 ratio) and dried. The protein standards are in the first lane (B). Individual lanes of the two gels correspond to the E/I ratios indicated. "−", no inhibitor.

of those noted as temporary inhibitors in Table 2, all eglin variants remained intact after this treatment (data not shown).

*Substitution of Arg at $P_2$ and $P_6$ Results in Temporary Inhibitors of Furin.* Both Kex2 and, to a lesser extent, furin, recognize basic residues at $P_2$ (*46*, *47*). In addition, furin interacts with Arg at $P_6$ (*48*). In an attempt to produce inhibitors of even higher affinity, Arg was introduced at $P_2$ and $P_6$. $R_6R_4R_1$-eglin was made by substituting Arg for $Gly_{40}$ in $R_4R_1$-eglin. $R_6R_4R_1$-eglin was a temporary inhibitor of furin: significant activity was recovered about 15 min after Boc-Arg−Val−Arg−Arg-MCA (2 $\mu$M) was added to an enzyme−inhibitor solution (data not shown). SDS−PAGE analysis coupled with N-terminal sequence analysis showed that recovery of activity was due to cleavage of the inhibitor carboxyl to the $P_1$ Arg ($Arg_{45}$, data not shown). The $K_a$ of furin for $R_6R_4R_1$-eglin could be determined during the initial inhibitory phase and did not differ significantly from the $K_a$ of furin for $R_4R_1$-eglin (Table 2 and Figure 5, panel C). In contrast, $R_6R_4R_1$-eglin formed a stable, stoichiometric complex with Kex2, again with an affinity similar to that of $R_4R_1$-eglin (Table 2).

Substitution at the $P_2$ position resulted in molecules that exhibited temporary inhibition of both furin and Kex2. These three eglin variants, $K_2R_1$-, $M_4K_2R_1$-, and $R_4K_2R_1$-eglin, initially inhibited both proteases, but reactions exhibited a slow, positive deviation from linearity. Once again, temporary inhibition was shown by SDS−PAGE (Figure 7) and N-terminal sequence analysis (data not shown) to be due to cleavage of the inhibitors after the $P_1$ Arg ($Arg_{45}$) and dissociation of the complex. $K_a$ values estimated from the linear part of reaction progress curves (Table 2) indicated that none of these eglin variants showed markedly increased affinity for either furin or Kex2. The fact, on one hand, that substitutions of Lys at $P_2$ resulted in a temporary inhibitor of both enzymes and, on the other hand, that substitution of Arg at $P_6$ created a temporary inhibitor of furin alone suggests that Lys at $P_2$ intrinsically affects the structure of the reactive

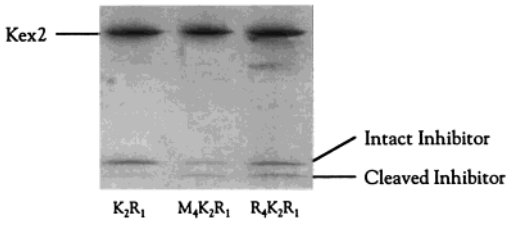


FIGURE 7: SDS−PAGE analyses of the reactions between Kex2 and three eglin variants that have the $Thr_{44}Lys$ substitution at ($P_2$). 64 pmol Kex2 was incubated with each eglin variant at a 1:1 molar ratio of enzyme to inhibitor for 5 h at 21 °C. Reactions were stopped with 10% TCA and subjected to PAGE analysis as described in the legend to Figure 6.

loop of the inhibitor, whereas, Arg at $P_6$ affects loop structure only when complexed with furin. This interpretation could be further tested by assessing the effect of substituting Ala for Thr at $P_2$ (see Discussion).

*Substitution of Lys at $P_1$ Differentially Affects Eglin Affinity for Furin and Kex2.* Two variants, $R_4K_1$-eglin and $M_4K_1$-eglin, were designed to examine the effect of substituting Lys for Arg at $P_1$. Furin exhibited a 15.4-fold reduced $K_a$ with $R_4K_1$-eglin, relative to $R_4R_1$-eglin (Table 2) but only a 4.7-fold decreased $K_a$ with $M_4K_1$-eglin as compared to $M_4R_1$-eglin (Table 2). In contrast, Kex2 exhibited only a 2.8-fold decrease in $K_a$ with $R_4K_1$-eglin relative to $R_4R_1$-eglin but exhibited a larger, 13.2-fold decrease in $K_a$ with $M_4K_1$-eglin relative to $M_4R_1$-eglin (Table 2). Thus, substitution of Lys for Arg at $P_1$ had a greater effect on furin affinity when Arg was present at $P_4$ but a greater effect on Kex2 affinity when Met was at $P_4$. Taken together, the quantitative analysis of affinities of the eglin variants for furin and Kex2 show that the two enzymes responded quite differently to substitutions at the $P_1$, $P_4$, and $P_6$ positions in the inhibitor.

*Inhibitor Association and Dissociation Rates.* For biological application of these eglin variants as inhibitors of processing in vivo, the rate of binding to target enzymes may be critical. Therefore, the rate of action of eglin variants with Kex2 and furin was examined by incubating $5 \times 10^{-10}$ M enzyme with inhibitor at molar ratios of inhibitor to enzyme ranging from 10 to 80. Typical progress curves (Figure 8, panel A) showed that $M_4R_1$-eglin was a slow, tight-binding inhibitor of Kex2. A similar progress curve was observed for furin inhibition with the $R_4R_1$-eglin. The relationship between $k_{obs}$ and inhibitor concentration was linear, as shown (Figure 8, panel B). $k_{on}$ values were determined from the slope of such curves, and dissociation rate constants ($k_{off}$) were calculated ($k_{off} = k_{on}/K_a$) (Table 3). For $R_4R_1$-eglin, $k_{off}$ was calculated to be $2 \times 10^{-4}$ s $^{-1}$ for Kex2, and $3 \times 10^{-4}$ $s^{-1}$ for furin (Table 3). Thus, the half-life ($t_{1/2}$) of the complex of $R_4R_1$-eglin with Kex2 and furin was estimated to be about 1 h. Similarly, the $t_{1/2}$ of the complex of $M_4R_1$-eglin with Kex2 was estimated to be 3 h. For complex of $R_4K_1$-eglin with furin, $k_{off}$ was calculated to be $2 \times 10^{-4}$ $s^{-1}$, implying that the $k_{off}$ and $t_{1/2}$ for this complex are similar to those for the complex of $R_4R_1$-eglin with furin.

*Inhibition of Other Serine Proteases by Eglin c Variants.* $L_1$-eglin inhibited subtilisin Carlsberg with a $K_a$ of $6.7 \times 10^{10}$ $M^{-1}$, human neutrophil elastase with a $K_a$ of $4.5 \times 10^{10}$ $M^{-1}$, and chymotrypsin with a $K_a$ of $1.1 \times 10^{10}$ $M^{-1}$ under our standard assay conditions. These $K_a$ values are consistent with those previously reported (*65*−*69*). The substitution of

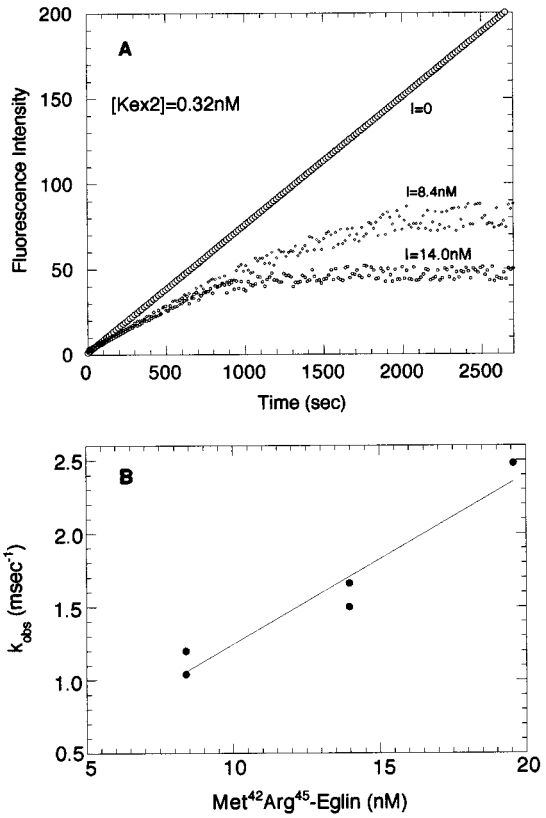


FIGURE 8: Determination of association rate constant ($k_{on}$) for inhibition of Kex2 (0.32 nM, E) with $M_4R_1$-eglin (I). Hydrolysis of Boc-Arg−Val−Arg−Arg-MCA was monitored for 45 min at room temperature. (A) The I/E ratios were 0, 18, and 44. Progress curves were analyzed graphically by fitting to eq 2. (B) $k_{obs}$, calculated from progress curves, was plotted versus the inhibitor concentration. $k_{on}$ values were calculated using eq 3 (Table 3).

Table 3: Experimentally Determined Association ($k_{on}$) and Calculated Dissociation ($k_{off}$) Rate Constants for Complexes Formed between Eglin Variants and Kex2 and Furin

| | $k_{on}$ ($M^{-1}s^{-1}$) | | $k_{off}$ ($s^{-1}$) | |
|---|---|---|---|---|
| eglin variant | Kex2 | furin | Kex2 | furin |
| $M_4R_1$- | $2 \times 10^5$ | nd[a] | $7 \times 10^{-5}$ | nd |
| $R_4R_1$- | $2 \times 10^5$ | $1 \times 10^5$ | $2 \times 10^{-4}$ | $3 \times 10^{-4}$ |
| $R_4K_1$- | nd | $5 \times 10^3$ | nd | $2 \times 10^{-4}$ |
| $R_6R_4R_1$- | $5 \times 10^5$ | nd | $1 \times 10^{-4}$ | nd |

[a] nd, not determined.

Arg for $Leu_{45}$ at $P_1$ almost completely abolished elastase inhibition (data not shown). However, $R_1$-eglin retained inhibitory activity against trypsin ($K_a = 1.8 \times 10^{10}$ $M^{-1}$) and subtilisin Carlsberg ($K_a = 1.0 \times 10^{10}$ $M^{-1}$) with affinities similar to those previously reported (*66*, *69*). Even though $R_4R_1$-eglin and $M_4R_1$-eglin were temporary inhibitors of trypsin, it was possible to determine $K_a$ values of $8.4 \times 10^9$ $M^{-1}$ and $4.4 \times 10^{10}$ $M^{-1}$, respectively, for the interaction of these two inhibitors with trypsin. $M_4R_1$-eglin inhibited subtilisin Carlsberg with a $K_a$ of $6.6 \times 10^{10}$ $M^{-1}$. Substitution of Arg at $P_4$ in $R_4R_1$-eglin reduced affinity for subtilisin ($K_a$ of $6.5 \times 10^8$ $M^{-1}$). Thus, subtilisin, unlike Kex2 and furin, exhibits interactions with eglin c that are largely insensitive to the identities of the $P_1$ and $P_4$ residues. Of greater relevance to the use of eglin c variants in cellular inhibition studies, we extended our inhibition studies to human plasma kallikrein and plasmin. $R_1$-eglin exhibited weak inhibition of these plasma proteases with $K_a$ values in the range of $10^6$ $M^{-1}$ (data not shown).

## DISCUSSION

Here we have shown that simple substitutions at $P_1$ and $P_4$, in the reactive site loop of eglin c yield high affinity (ca. nanomolar) inhibitors of the processing proteases furin and Kex2. These inhibitors have several advantageous characteristics that should make them useful for both biochemical and cell-based experiments. Like wild-type eglin c, the engineered molecules are small, stable proteins lacking disulfide bonds that are easy to express and purify in large quantities in bacterial cultures. In general, these inhibitors form stable, stoichiometric complexes with furin and Kex2 that do not undergo enzymatic turnover. Moreover, the complex of furin with $R_4R_1$-eglin is stable over a physiological pH range, from at least 6.0 to 7.4, suggesting that inhibitory complexes formed at the cell surface should remain intact after endocytic internalization (see below). Although high-affinity inhibitors are desired for applications such as cocrystallization or cellular inhibition, we have found that the more modest inhibitors are also useful in creation of affinity purification resins (T. Komiyama and R. S. Fuller, unpublished results).

Several of the eglin variants described in this study exhibit significant selectivity between the two processing proteases studied, furin and Kex2. Selectivity is evident in the differential effects of substitutions at $P_1$, $P_4$, and $P_6$ in eglin c on the two enzymes. In the case of $P_1$, for example, $R_4K_1$-eglin exhibited ~20-fold higher affinity for Kex2 than for furin, whereas, Kex2 bound $R_4R_1$-eglin only ~3-fold more strongly than furin did. The most striking case of selectivity was seen at $P_4$, where Kex2 exhibited ~10 000-fold higher affinity for $M_4R_1$-eglin than did furin. This finding is consistent with the dual specificity (aliphatic or basic) exhibited by Kex2 in $P_4$ recognition (ref *51*; D. J. Krysan and R. S. Fuller, unpublished results) and also with the contrastingly stringent requirement by furin for Arg at $P_4$ (*48*). A different kind of selectivity was observed at $P_6$. Although introduction of Arg at $P_6$ failed to result in significant enhancement of affinity for either enzyme, in the case of furin, $R_6R_4R_1$-eglin was a temporary inhibitor, whereas, the same molecule formed a stable complex with Kex2. We interpret this in light of evidence that introduction of Arg at $P_6$ in peptide substrates enhances catalysis by furin (~10-fold $k_{cat}/K_M$) but has a negligible effect on Kex2 activity. Thus, we conclude that it is the interaction between furin and the $P_6$ Arg side chain, rather than an intrinsic effect of the Arg on the conformation of the reactive site loop, that is responsible for the fact that $R_6R_4R_1$-eglin becomes a substrate for furin. The interaction of furin with the Arg at $P_6$ in $R_6R_4R_1$-eglin presumably alters the conformation of the loop so that it can be cleaved by the enzyme. Kex2, which fails to interact with the $P_6$ Arg, does not perturb the loop conformation and therefore forms a stable complex. Selectivity was also apparent in the degree of cooperativity observed in interactions with the $P_1$ and $P_4$ side chains. Previous studies of Kex2 and furin using small peptide substrates demonstrated energetic cooperativity between $P_1$ and $P_4$ (*48*, *51*). Such cooperativity is evident in the interactions of both enzymes with the eglin variants but is much greater in the case of furin where $R_4R_1$-eglin exhibited ~5.5 kcal/mol

greater relative binding energy than would be predicted by the sum of the relative binding energies of $R_1$-eglin and $R_4$-eglin.[2]

In the crystal structure of eglin c, the $\beta$-hydroxyl of $Thr_{44}$ ($P_2$) is part of a hydrogen bond network with the side chains of $Arg_{53}$ and $Asp_{46}$ (*40*, *69*−*71*). These interactions are thought to be important for maintaining the rigidity of the reactive site loop and indeed, in the crystal structures of complexes between eglin c and subtilisins, the conformation of the reactive site loop is essentially identical to that in the structure of eglin c alone. There is no contact between the $Thr_{44}$ side chain and the $S_2$ subsite of the enzymes in cocrystals. Chymotrypsin inhibitor 2 (CI2), another member of the potato inhibitor 1 family and thus homologous to eglin c, like eglin c also exhibits strong, stable inhibition of subtilisins. Similar to effects we observed of substitutions at the $P_2$ position of eglin c, substitution of Ala or Asp for Thr at the $P_2$ position in the reactive site loop of CI2 converted CI2 into a temporary inhibitor of subtilisin BPN′ (*64*). The inhibitory activity of CI2 declined and stability of the complex of CI2-subtilisin BPN′ decreased. Jackson and Fersht concluded that Thr at $P_2$ plays an important role in stabilizing the reactive site loop of CI2 (*64*). Furthermore, Thr is also found at $P_2$ in the reactive site loop of protease inhibitors belonging to evolutionarily distinct families where it plays a role in loop stabilization (*34*, *71*). Substitution of Lys for $Thr_{44}$ in $M_4K_2R_1$-eglin and $R_4K_2R_1$-eglin resulted in temporary inhibitors for both Kex2 and furin, consistent with the notion that the $Lys_{44}$ substitution disrupts interactions that ordinarily stabilize the reactive site loop. However, interaction between $Lys_{44}$ and the $S_2$ subsite of Kex2 and furin might also contribute to temporary inhibition. The relative importance of loop destabilization and $P_2$−$S_2$ interaction in the temporary inhibition by the $Lys_{44}$ variants could be tested by evaluating the effect of substituting Ala for $Thr_{44}$. This substitution would eliminate the hydrogen-bonding interactions of $Thr_{44}$ that stabilize the loop without introducing a side chain that could interact with the target enzyme.

Previous experiments with the serpin, $\alpha_1$-antitrypsin, demonstrated that introduction of Arg in the reactive site loop at positions equivalent to $P_1$ and $P_4$ converted a molecule without measurable affinity for furin into a selective furin inhibitor, $\alpha_1$-PDX, with a $K_i$ in the nanomolar range (*30*). Here we have found that similar substitutions in eglin c, an inhibitor of a different family, resulted in a 46 000-fold increase in affinity for human furin and even more impressive 550 000-fold increase in affinity for yeast Kex2 protease, resulting in an inhibitor with approximately nanomolar affinity for each enzyme. In contrast, in the case of the turkey ovomucoid third domain inhibitor, substitution of Arg at $P_1$ and $P_4$ along with Lys at $P_2$ only resulted in an inhibitor with a $K_a$ of $\sim 10^7$ $M^{-1}$ (*29*), making the point that protease inhibitor families are not likely to be equally adaptable to all target enzymes. Although eglin c presumably evolved to form tight complexes with mammalian proteases such as neutrophil elastase (*35*), the fact that the inhibitor was known to form tight complexes with subtilisins made eglin c an attractive candidate for engineering processing enzyme inhibitors. Although selectivity of $R_4R_1$-eglin for furin relative to other mammalian processing enzymes of the kexin/furin family has not yet been tested, eglin c-based inhibitors clearly have several attractive features: (i) small size, (ii) ease of expression and purification, (iii) lack of disulfide bonds, and (iv) high thermal stability.

Efficacy of eglin variants in cellular inhibition of processing remains to be tested. In the case of $\alpha_1$-PDX, experiments show that inhibition in cells can be achieved either by intracellular expression or by addition of purified protein to cell cultures. Work by Thomas and colleagues suggests that exogenous $\alpha_1$-PDX most likely inhibits by binding furin at the cell surface. Over the course of 6 h, essentially all furin molecules cycle through the plasma membrane and become inactivated and undergo down-regulation, presumably by lysosomal degradation (*72*). Such down-regulation may or may not be a feature of serpin−enzyme complexes that will not be seen with eglin c-based inhibitors. However, eglin c-based inhibitors may have an advantage by virtue of their reversibility.

The substitutions made in eglin at $P_2$ and $P_6$ represented attempts to generate even higher-affinity inhibitors for furin and Kex2, but these substitutions did not have the desired effects. Substitutions at $P_1$, $P_2$, $P_4$, and $P_6$ exhaust the possibilities to optimize substrate-like contacts between eglin c and the processing proteases. To obtain further improvements in affinity, it will be necessary to optimize other interactions. One approach is to optimize adventitious interactions between the enzyme and the inhibitor at positions lateral to the active site/reactive site loop interface. Preliminary results suggest that such sites can be identified by screening variants produced by randomizing specific residues in the eglin template outside the reactive site loop. Variants of $R_4R_1$-eglin have been obtained in this manner that exhibit affinities up to 15-fold higher than seen with $R_4R_1$-eglin itself (T. Komiyama, B. VanderLugt, and R. S. Fuller, unpublished data). Combining advantageous substitutions may produce even higher affinities. Furthermore, randomizing adventitious interactions may also provide the basis for evolving inhibitor molecules that are selective for different members of the family of human processing enzymes. This is important because these enzymes exhibit rather similar specificities at $P_1$, $P_2$, and $P_4$. Eglin c can thus be viewed as a common chassis on which to build highly selective, high-affinity inhibitors for each of the human processing proteases.

## ACKNOWLEDGMENT

An $Arg_{45}$-eglin c chemically synthesized with Cys at the $P_5$ position was a gift of Wuyuan Lu (University of Chicago). We tested the $Cys_{41}Arg_{45}$-eglin inhibition of Kex2 previously to the present study. We thank Ron Taussig for generous help with Bacuolovirus expression and insect cell culture. We also thank the University of Michigan DNA and Protein Core Facilities for oligonucleotide synthesis, DNA sequencing, N-terminal sequencing, isoelectric focusing-PAGE, and MALDI mass spectroscopy. We thank Jack Thomas for preparation of Kex2 and pFast Bac fur-595 DNA. Thanks to members of the Fuller lab for helpful suggestions on the manuscript and stimulating discussion. We thank members of David Engelke's lab and Dennis Thiele's lab (University of Michigan) for sharing expertise and facilities.

[2] $\Delta\Delta G°_{R_4R_1/WT} = 6.4$ kcal/mol, the difference between $\Delta G°$ for binding eglin c having the wild-type loop and $\Delta G°$ for binding eglin c having the $R_4R_1$ loop. Similarly, $\Delta\Delta G°_{R_1/WT} = 0.46$ kcal/mol and $\Delta\Delta G°_{R_4/WT} = 0.43$ kcal/mol.

## REFERENCES


1. Zhou, A., Webb, G., Zhu, X., and Steiner, D. F. (1999) *J. Biol. Chem. 274*, 20745−20748.
2. Fuller, R. S., Sterne, R. E., and Thorner, J. (1988) *Annu. Rev. Physiol. 50*, 345−362.
3. Furuta, M., Carroll, R., Martin, S., Swift, H. H., Ravvazzola, M., Orei, L., and Steiner, D. F. (1998) *J. Biol. Chem. 273*, 3431−3437.
4. Furuta, M., Zhou, A., Rouille, Y., Holst, J. J., Carroll, R., Ravazzola, M., Orci, L., Furuta, H., and Steiner, D. F. (1997) *Proc. Natl. Acad. Sci. U.S.A. 94*, 6646−6651.
5. Jackson, R. S., Creemers, J. W., Ohagi, S., Raffin-Sanson, M. L., Snaders, L., Montague C. T., Hutton, J. C., and O'Rahilly, S. (1997) *Nat. Genet. 16*, 303−306.
6. Roebroek, A. J. M., Umans, L., Pauli, I. G. L., Robertson, E. J., van Leuven, F., Van de Ven, W. J. M., and Constam, D. B. (1998) *Development 125*, 4863−4876.
7. Molloy, S. S., Anderson, E. D., Jean, F., Thomas, G. (1999). *Trends Cell Biol. 9*, 28−35.
8. Molloy, S. S., Bresnaham, P. A., Leppla, S. H., Klimpel, K. R., and Thomas, G. (1992). *J. Biol. Chem. 267*, 16396−16402.
9. Chiron, M. F., Fryling, C. M., and FitzGerald, D. J. (1994) *J. Biol. Chem. 269*, 18167−18176.
10. Inocencio, N. M., Moehring, J. M., and Moehring, T. J. (1994)- *J. Biol. Chem. 269*, 31831−31835.
11. Garred, O., Deurs, B., and Sandvig, K. (1994) *J. Biol. Chem. 270*, 10817−10821.
12. Sariola, M., Saraste, J., and Kuismanen, E. (1995) *J. Cell Sci. 106*, 2465−2475.
13. Moehring, J. M., Inocencio, N. M., Robertson, B. J., and Moehring, T. J. (1993) *J. Biol. Chem. 268*, 2590−2594.
14. Ortmann, D., Ohuchi, M., Angliker, H., Shaw, E., Garten, W., and Klenk, H.-D. (1994) *J. Virol. 68*, 2772−2776.
15. Stieneke-Grober, A., Vey, M., Angliker, H., Shaw, E., Thomas, G., Roberts, C., Klenk, H.-D., and Garten, W (1992) *EMBO J. 11*, 2407−2414.
16. Hallenberger, S., Bosch, V., Angliker, H., Shaw, E., Klenk, H. D., and Garten, W. (1992) *Nature 360*, 358−361.
17. Gao, P., Watanabe, S., Ito, T., Goto, H., Wells, K., McGregor, M., Cooley, A. J., and Kawaoka, K. (1999) *J. Viol. 73*, 3184−3189.
18. Bolt, G., and Pedersen, I. R. (1998) *Virology 252*, 387−398.
19. Volchkov, V. E., Feldmann, H., Volchkova, V. A., and Klenk, H. D. (1998) *Proc. Natl. Acad. Sci. U.S.A. 95*, 5762−5767.
20. Richt, J. A., Furbringer, T., Kock, A., Pfeuffer, I., Herden, C., Bause-Niedrig, I., and Gaten, W. (1998) *J. Virol. 72*, 4528−4533.
21. Watanabe, M., Hirano, A., Stenglein, S., Nelson, J., Thomas, G., and Wong, T. C. (1995) *J. Virol. 69*, 3206−3210.
22. Vey, M., Yano, H., Schafer, W., Reis, B., Ohuchi, R., Britt, W., Garten W., Klenk, H. D., and Radsak, K. (1995) *Virology 206*, 746−749.
23. Stadler, K., Allison, S. L., Schalich, J., and Heinz, F. X. (1997)- *J. Viol. 71*, 8475−8481.
24. Robertson, B. J., Moehring, J. M., and Moehring, T. J. (1993) *J. Biol. Chem. 268*, 24274−24277.
25. Takahashi, S., Kasai, K., Hatsuzawa, K., Kitamura, N., Misumi, Y., Ikehara, Y., Murakami, K., and Nakayama, K. (1993) *Biochem. Biophys. Res. Commun. 195*, 1019−1026.
26. Angliker, H., Wikstrom, P., Shaw, E., Brenner, C., and Fuller, R. S. (1993) *Biochem. J. 293*, 75−81.
27. Angliker, H. (1995) *J. Med. Chem. 38*, 4014−4018.
28. Garten, W., Hallenberger, S., Ortmann, D., Schafer, W., Vey, M., Angliker, H., Shaw, E., and Klenk, H. D. (1994) *Biochimie 76*, 217−225.
29. Lu, W., Zhang, W., Molloy, S. S., Thomas, G., Ryan, K., Chiang, Y., Anderson, S., and Laskowski, M., Jr. (1993) *J. Biol. Chem. 268*, 14583−14585.
30. Jean, F., Stella, K., Thomas, L., Liu, G., Xiang, Y., Reason, A., and Thomas, G. (1998) *Proc. Natl. Acad. Sci. U.S.A. 95*, 7293−7298.
31. Dahlen, J. R., Jean, F., Thomas, G., Foster, D. C., and Kisiel, W. (1998) *J. Biol. Chem. 273*, 1851−1854.
32. Oda, K., Takahashi, S., Kikuchi, N., and Shibano, Y. (1996) *Biosci. Biotechnol. Biochem. 60*, 1388−1389.
33. Anderson, E. D., Thomas, L., Hayflick, J. S., and Thomas, G. (1993) *J. Biol. Chem. 268*, 24887−24891.
34. Laskowski, M., Jr., and Kato, I. (1980) *Annu. Rev. Biochem. 49*, 593−626.
35. Seemüller, U., Dodt, J., Fink, E., and Fritz, H. (1986) in *Proteinase Inhibitors* (Barret, A. J., and Salvesen, G., Eds.) pp 336−359, Elsevier, Amsterdam.
36. Bode, W., and Huber, R. (1992) *Eur. J. Biochem. 204*, 433−451.
37. Greagg, M. A., Brauer, A. B. E., and Leatherbarrow, R. J. (1994) *Biochim. Biophys. Acta 1222*, 179−186.
38. Bae, S.-J., and Sturtevant, J. M. (1995) *Biophys. Chem. 55*, 247−252.
39. McPhalen, C. A., Schnebli, H. P., and James, M. N. G. (1985) *FEBS Lett. 188*, 55−58.
40. Bode, W., Papamokos, E., Musil, D., Seemüller, U., and Fritz, H. (1986) *EMBO J. 5*, 813−818.
41. Dauter, Z., Betzel, C., Genov, N., Pipon, N., and Wilson, K. S. (1991) *Acta Crystallogr. B47*, 707−730.
42. Gros, P., Betzel, Ch., Dauter, Z., Wilson, K. S., and Hol, G. J. (1989) *J. Mol. Biol. 210*, 347−367.
43. Li, A., and V. Daggett, V. (1995) *Protein Eng. 8*, 1117−1128.
44. Hyberts, S. G., Goldberg, M. S., Havel, T. F., and Wagner, G. (1992) *Protein Sci. 1*, 736−751.
45. Brenner, C., and Fuller, R. S. (1992) *Proc. Natl. Acad. U.S.A. 89*, 922−926.
46. Bravo, D. A., Gleason, J. B., Sanchez, R. I., Roth, R. A., and Fuller, R. S. (1994) *J. Biol. Chem. 269*, 25830−25837.
47. Rockwell, N. C., Wang, G. T., Krafft, G. A., and Fuller, R. S. (1997) *Biochemistry 36*, 1912−1917.
48. Krysan, D. J., Rockwell, N. C., and Fuller, R. S. (1999) *J. Biol. Chem. 36*, 23229−23234.
49. Grøn, H., Meldal, M., and Breddam, K. (1992) *Biochemistry 31*, 6011−6018.
50. Grøn, H., and Breddam, K. (1992) *Biochemistry 31*, 49−53.
51. Rockwell, N. C., and Fuller, R. S. (1998) *Biochemistry 37*, 3386-3391.
52. Watanabe, T. K., Murakami, T. K., and Nakayama, K. (1993) *FEBS Lett. 320*, 215−218.
53. Brenner, C., Bevan, A., and Fuller, R. S. (1994) *Methods Enzymol. 244*, 152−167.
54. Sambrook, J., Fritsch, E. F., Maniatis, T. (1989) *Molecular Cloning*, Cold Spring Harbor Laboratory Press, New York.
55. Rink, H., Liersch, M., Sieber, P., and Meyer, F. (1984) *Nucleic Acid Res. 12*, 6369−6387.
56. Hanahan, D., Jessee, J., and Bloom, F. R. (1995) in *DNA Cloning 1* (Glover, D. M., and Hames, B. D., Eds.) pp 1−36, IRL Press, Oxford.
57. Bury, A. (1981*) J. Chromat. 213*, 491−500.
58. Goldenberg, D. P. (1989) in *Protein Structure* (Creighton, T. E., Ed.) pp 225−250, IRL Press, Oxford.
59. Komiyama, T., Grøn, H., Pemberton, P. A., and Salvesen, G. S. (1996) *Protein Sci. 5*, 874−882.
60. Matsudaira, P. (1987) *J. Biol. Chem. 262*, 10035−10038.
61. Chase, T., and Shaw, E. (1969) *Biochemistry 8*, 2212−2224.
62. Green, N. M., and Work, E. (1953) *Biochem. J. 54*, 347−352.
63. Knight, C. G. (1986) in *Proteinase Inhibitors* (Barrett, A. J., and Salvesen, G., Eds.) pp 23−51, Elsevier, Amsterdam.
64. Jackson, S. E., and Fersht, A. R. (1993*) Biochemistry 32*, 13909−13916.
65. Braun, N. J., Bodmer, J. L., Virca, G. D., Metz-Virca, G., Maschler, R., Bieth, J. G., and Schnelbi, H. P. (1987) *Biol. Chem. Hoppe-Seyler 368*, 299−308.
66. Heinz, D. W., Priestle, J. P., Rahuel, J., Wilson, K. S., and Grütter, M. G. (1991) *J. Mol. Biol. 217*, 353−371.
67. Ascenzi, P., Aducci, P., Amiconi, G., Ballio, A., Guaragna, A., Menegatti, E., Schnebli, H. P., and Bolognesi, M. (1991*) J. Mol. Recogn. 4*, 113−119.

68. Qasim, M. A., Ganz, P. J., Saunders, C. W., Bateman, K. S., James, M. N. G., and Laskowski, M., Jr. (1997) *Biochemistry 36*, 1598−1607.
69. Lu, W., Randal, M., Kossiakoff, A., and Kent, S. B, H. (1999) *Chem. Biol. 6*, 419−427.
70. McPhalen, C. A., and James, M. N. G. (1988) *Biochemistry 27*, 6582−6598.
71. McBride, J. D., Brauer, A. B. E., Nievo, M., and Leatherbarrow, R. L. (1998) *J. Mol. Biol. 282*, 447−457.
72. Jean, F., Thomas, L., Molloy, S. S., Liu, G., Jarvis, M. A., Nelson, J. A., and Thomas, G. (2000) *Proc. Natl. Acad. Sci. U.S.A. 97*, 2864−2869.

BI001907C